

March 22, 2015

# On the change in helix handedness at transitions between the $\text{SmC}^*$ and $\text{SmC}_a^*$ phases in chiral smectic liquid crystals

Jan P. F. Lagerwall<sup>1\*</sup>, Frank Giesselmann<sup>1</sup>, and Mikhail Osipov<sup>2</sup>

<sup>1</sup>*Institute of Physical Chemistry, University of Stuttgart,  
Pfaffenwaldring 55, D-70569 Stuttgart, Germany*

<sup>2</sup>*Department of Mathematics, University of Strathclyde, Glasgow, Scotland (UK)*

## Abstract

Using a discrete model for the synclinic  $\text{SmC}^*$  and the anticlinic  $\text{SmC}_a^*$  phases we give the theoretical explanation to the fact that the helix twisting sense reverses at a transition between these phases (direct transition or via the so-called chiral smectic-C 'subphases') and we derive an explicit expression for the helical pitch in the  $\text{SmC}_a^*$  phase. As the theory shows and as we also demonstrate experimentally, the reversal is of a different nature than helix inversions within a single phase, where the inversion is always coupled to a pitch divergence. At a clinicity change the common behavior is instead pitch shortening on approaching the phase transition and the associated helix twisting sense reversal. The phenomenon may be put to use in smart mixing in order to control the helix pitch, either for achieving long pitch for surface-stabilised ferroelectric (FLC) and antiferroelectric liquid crystal (AFLC) displays, or a very short pitch, in case of devices utilising the deformed helix mode.

---

\* E-mail for correspondence: [jan.lagerwall@ipc.uni-stuttgart.de](mailto:jan.lagerwall@ipc.uni-stuttgart.de)  
Fax: 0049 711 684 2569  
Telephone: 0049 711 685 4458

## I. INTRODUCTION

It is an empirically well established fact that the helical superstructures of the  $\text{SmC}^*$  and  $\text{SmC}_a^*$  phases, when they both occur in the same substance, have opposite handedness [1–3], but no attempts have to our knowledge been made at explaining it theoretically. Here we give such an explanation, using a discrete phenomenological model, and we demonstrate experimentally, using mixtures of strictly syn- and anticlinic compounds (forming no other smectic-C-type phase than  $\text{SmC}^*$  and  $\text{SmC}_a^*$ , respectively), that the helix sense reversal is of a quite different nature than helix inversions within one and the same phase. We finally discuss how the phenomenon may be useful when developing mixtures for devices based on ferroelectric (FLC) or antiferroelectric liquid crystals (AFLCs).

## II. THE ORIGIN OF THE HELICAL TWISTING SENSE REVERSAL AT THE SMECTIC-C\*–SMECTIC-C<sub>a</sub>\* TRANSITION

In this section we show that the change in handedness of the helical structure at a transition from synclitic  $\text{SmC}^*$  to anticlinic  $\text{SmC}_a^*$  is generally a result of the clinicity change itself. Thus it should be a general phenomenon not related to a particular molecular structure, at least in one-component systems (the observations described in the experimental section show, however, that it holds also for binary mixtures). We first consider a very simple model which enables one to demonstrate the origin of the effect, and then we derive more general expressions for the helical pitch in the  $\text{SmC}^*$  and  $\text{SmC}_a^*$  phases, respectively, which can be compared directly because they depend on the same parameters of the model.

### A. A simple discrete model

In the discrete model the free energy  $F$  of a smectic phase per unit area of the layers is expressed as a sum over all layers :

$$F = \sum_j F_j, \quad (1)$$

where the  $F_j$  depend on the order parameters for individual layers  $j$ . In the simplest case one may consider only the tilting order parameter [4–6]

$$\mathbf{w}_j = (\mathbf{n} \cdot \mathbf{k})(\mathbf{n} \times \mathbf{k}) \quad (2)$$

where  $\mathbf{n}$  is the director and  $\mathbf{k}$  is the unit vector in the direction perpendicular to the smectic layers (the smectic layer normal). The magnitude of the tilting order parameter  $|\mathbf{w}_j| = w_0 = (1/2)\sin 2\Theta$  where  $\Theta$  is the tilt angle and its direction is perpendicular to the tilt plane. Now the free energy can be expressed in terms of simple invariants composed of the pseudovectors  $\mathbf{w}_j$  and the layer normal  $\mathbf{k}_0$  [7, 8]:

$$F = \sum_j F_0(w_j^2) - \frac{1}{2}\eta(\mathbf{w}_j \cdot \mathbf{w}_{j+1}) - \lambda(\mathbf{w}_j \times \mathbf{w}_{j+1} \cdot \mathbf{k}_0). \quad (3)$$

Here  $F_0$  is the internal free energy of any single layer and the last two terms in eq. (3) describe the orientational coupling between adjacent layers. This coupling is expressed taking into account only terms quadratic in  $\mathbf{w}_j$ . The second term describes the nonchiral orientational coupling while the third term is present only in chiral systems. The coefficient  $\lambda$  is a pseudoscalar which is determined by molecular chirality.

It is well known that the simple model (3) can be used to describe the transition between the synclinc and the anticlinc phase [9–11]. Indeed, as  $(\mathbf{w}_j \cdot \mathbf{w}_{j+1})$  is positive in the synclinc but negative in the anticlinc case, we see that the synclinc structure is stable if the parameter  $\eta > 0$  while the anticlinc structure is stable if  $\eta < 0$ . The third (chiral) term induces the helical structure in both phases, and one can express the helical pitch in the synclinc and the anticlinc phases in terms of the model parameters  $\lambda$  and  $\eta$ . Again, the sense of the helix is determined by the structure that corresponds to a negative third term in (3).

One can then readily understand the origin of the sense reversal at the synclinc–anticlinc transition using the following simple qualitative argument. Let us assume that the z-axis is perpendicular to the smectic layers and that the tilt order parameter  $\mathbf{w}_j$  in the layer  $j$  is parallel to the x-axis, i.e.  $\mathbf{w}_j = w_0(1, 0, 0)$ . In the SmC\* phase with helical structure the tilt order parameter  $\mathbf{w}_{j+1}$  in the adjacent layer  $j + 1$  can be expressed as  $\mathbf{w}_{j+1} = w_0(\cos qd, \sin qd, 0)$  where  $q$  is the wave vector of the helical structure and  $d$  is the layer spacing. The non-helical case  $\mathbf{w}_j = \mathbf{w}_{j+1}$  corresponds to the limit  $q = 0$ . Substituting these expressions into the third term in eq. (3) one obtains  $-\lambda(\mathbf{w}_j \times \mathbf{w}_{j+1} \cdot \mathbf{k}_0) = -\lambda w_0^2 \sin qd$ , which for a positive  $\lambda$  renders  $q > 0$  in SmC\*.

Now one may assume that in the anticlinc SmC<sub>a</sub>\* phase the tilt order parameter  $\mathbf{w}_j$  is antiparallel to the x-axis in the layer  $j$ , i.e.  $\mathbf{w}_j = w_0(-1, 0, 0)$ . In the layer  $j + 1$  the tilt order parameter  $\mathbf{w}_{j+1}$  is given by the same expression as before. In this case we instead find

that  $-\lambda(\mathbf{w}_j \times \mathbf{w}_{j+1} \cdot \mathbf{k}_0) = +\lambda w_0^2 \sin qd$ . Thus the 'helical twisting power' term in the free energy of the anticlinic  $\text{SmC}_a^*$  phase is negative only if  $q$  is negative (since we have assumed  $\lambda > 0$ ), i.e. the twisting sense is opposite to that of the synclinic  $\text{SmC}^*$  phase. This simple argument will be made more quantitative in the following sections.

### 1. Synclinic $\text{SmC}^*$ phase

In the helical  $\text{SmC}^*$  phase the tilting order parameter  $\mathbf{w}_j(z)$  can be expressed as

$$\mathbf{w}_j = \mathbf{w}(z_j) = w_0 (\cos qz_j, \sin qz_j, 0), \quad (4)$$

where  $q$  is the wave vector of the helical structure,  $w_0 = (1/2) \sin 2\Theta$  and  $z_j = dj$  where  $d$  is the layer spacing. The vector  $\mathbf{w}(z)$  slowly rotates along the  $z$ -axis thus describing the helix. The pitch of the helical structure  $p = 2\pi/q$  is always much larger than the layer spacing  $d$ , and therefore the free energy can be expanded in powers of  $qd$  keeping the lowest order terms. In particular, the order parameter in the layer  $j + 1$  can be expanded around its value in the adjacent layer  $j$  up to the quadratic term in  $q$ :

$$\mathbf{w}_{j+1} = \mathbf{w}_j + d \frac{\partial}{\partial z_j} \mathbf{w}_j + \frac{1}{2} d^2 \frac{\partial^2}{\partial z_j^2} \mathbf{w}_j + \dots \quad (5)$$

It can readily be shown using eq. (4) that

$$\frac{\partial^2}{\partial z_j^2} \mathbf{w}_j = -q^2 \mathbf{w}_j,$$

$$(\mathbf{w}_j \cdot \frac{\partial}{\partial z_j} \mathbf{w}_j) = 0 \quad (6)$$

$$\text{and } \frac{\partial}{\partial z_j} \mathbf{w}_j \times \mathbf{k}_0 = q \mathbf{w}_j.$$

Using these results one obtains:

$$(\mathbf{w}_j \cdot \mathbf{w}_{j+1}) \approx w_0^2 (1 - \frac{1}{2} q^2 d^2); \quad (7)$$

$$(\mathbf{w}_j \times \mathbf{w}_{j+1} \cdot \mathbf{k}_0) \approx w_0^2 qd.$$

Substituting eq. (7) into eq. (3) and dividing by the number of layers  $N$ , one thus obtains the free energy density

$$F/N = F_0(\Theta) + \frac{w_0^2}{N} \left( -\frac{\eta}{2} + \frac{\eta q^2 d^2}{4} - \lambda qd \right), \quad (8)$$

where we have introduced  $F_0(\Theta)$  for the component not related to interactions between layers. Now the wave vector  $q$  of the helical structure can be found by minimization of the free energy (8):

$$q = +\frac{2\lambda}{d\eta}. \quad (9)$$

## 2. Anticlinic $\text{SmC}_a^*$ phase

In the helical anticlinic  $\text{SmC}_a^*$  phase the (discrete) order parameter  $\mathbf{w}(z_j)$  can be written in the form

$$\mathbf{w}(z_j) = w_0 (\cos(\pi/d + q)z_j, \sin(\pi/d + q)z_j, 0). \quad (10)$$

Indeed, in the untwisted state ( $q = 0$ ) the  $y$  component of  $\mathbf{w}_j$  vanishes for all  $j$  and the  $x$ -component  $w_{j,x} = w_0 \cos(\pi/d)z_j = w_0 \cos(\pi j)$  oscillates in sign from layer to layer describing the anticlinic structure.

Using eq. (10) and the relation  $z_j = dj$  the order parameter of the anticlinic phase in the layer  $j + 1$  can be expressed as:

$$\mathbf{w}_{j+1} = -w_0 (\cos(\pi j + qz_j + qd), \sin(\pi j + qz_j + qd), 0). \quad (11)$$

Expanding eq. (11) in powers of  $qd$  up to the second order one obtains

$$\begin{aligned} \mathbf{w}_{j+1} &\approx -\mathbf{w}_j - (qd)w_0 (-\sin(\pi j + qz_j), \cos(\pi j + qz_j), 0) \\ &\quad + \frac{1}{2}(qd)^2 (\cos(\pi j + qz_j), \sin(\pi j + qz_j), 0) + \dots \\ &= -\mathbf{w}_j - d\frac{\partial}{\partial z_j}\mathbf{w}_j - \frac{1}{2}d^2\frac{\partial^2}{\partial z_j^2}\mathbf{w}_j + \dots \end{aligned} \quad (12)$$

One notes that the expansion (12) is similar to eq. (5) but with the negative sign. This negative sign is determined by that of the scalar product of the antiparallel order parameters  $\mathbf{w}_j$  and  $\mathbf{w}_{j+1}$  in adjacent layers in the anticlinic structure.

Exactly in the same way as in the case of the synclinc  $\text{SmC}^*$  phase the expansion (12) can be used to obtain equations similar to eqs. (7), but with the opposite sign:

$$(\mathbf{w}_j \cdot \mathbf{w}_{j+1}) \approx -w_0^2(1 - \frac{1}{2}(qd)^2) \quad (13)$$

$$(\mathbf{w}_j \times \mathbf{w}_{j+1} \cdot \mathbf{k}_0) \approx -w_0^2qd$$

Substituting eqs. (13) into eq. (3) one obtains the expression for the free energy of the anticlinic phase as a function of  $q$

$$F_a/N = F_0(\Theta) + \frac{w_0^2}{N} \left( \frac{\eta}{2} - \frac{\eta q^2 d^2}{4} + \lambda q d \right). \quad (14)$$

Minimization of the free energy (14) yields the expression for the wave vector of the helical structure in the anticlinic phase:

$$q = \frac{2\lambda}{d\eta} = -\frac{2\lambda}{d|\eta|}. \quad (15)$$

Note that the parameter  $\eta$  is negative within the stability range of the anticlinic phase, hence the sign of  $q$  in eq. (15) is opposite compared with the corresponding  $q$  in eq. (9) for the synclinic phase, for which  $\eta$  is positive. Thus the sense of the helical structure in the anticlinic  $\text{SmC}_a^*$  phase is opposite to that of the synclinic  $\text{SmC}^*$  phase. One notes that this sign reversal is simply a consequence of the fact that in the anticlinic phase the director tilts in opposite directions in neighboring layers.

It should be pointed out, however, that the model used so far is oversimplified because the spontaneous polarization  $\mathbf{P}$  is taken into account neither in the synclinic nor in the anticlinic phase in the model (3). It is well known from the general Landau-de Gennes theory of the ferroelectric  $\text{SmC}^*$  phase that the coupling between polarization and the tilting order parameter makes an additional contribution to the pitch. In the following two subsections we show that the same expressions for the pitch can also be obtained using a more general discrete model. The same approach will also be used to derive a general expression for the pitch in the anticlinic  $\text{SmC}_a^*$  phase.

## B. Relation between continuum and discrete approaches in the theory of the $\text{SmC}^*$ phase

In the general continuum approach the free energy density of the ferroelectric  $\text{SmC}^*$  phase can be written as [4–6]:

$$F = F_0(\Theta) + \frac{1}{2}K\nabla^2\mathbf{w} + \frac{1}{2}\chi^{-1}P^2 + \mu_p(\mathbf{w} \cdot \mathbf{P}) + \mu_f(\mathbf{P} \cdot \text{curl}\mathbf{w}) + \Lambda(\mathbf{w} \cdot \text{curl}\mathbf{w}), \quad (16)$$

where  $K$  is the elastic constant,  $\chi$  a generalized susceptibility,  $\mu_p$  and  $\mu_f$  the piezo- and flexoelectric coefficients, respectively,  $\Lambda$  a chiral parameter which induces the helical structure, and the order parameter  $\mathbf{w}$  is given by eq. (2). Only lower order terms in  $\Theta$  have here been taken into account. Assuming that both variables in eq. (16) depend only on  $z$ , the free energy density can be rewritten in the form

$$F = F_0(\Theta) + \frac{1}{2}K \frac{\partial^2}{\partial z^2} \mathbf{w} + \frac{1}{2}\chi^{-1}P^2 + \mu_p(\mathbf{w} \cdot \mathbf{P}) + \mu_f(\mathbf{P} \cdot \mathbf{k}_0 \times \frac{\partial}{\partial z} \mathbf{w}) + \Lambda(\mathbf{w} \cdot \mathbf{k}_0 \times \frac{\partial}{\partial z} \mathbf{w}). \quad (17)$$

After minimizing the free energy (17) with respect to the polarization  $\mathbf{P}$  and the wave vector of the helical structure  $q$  one obtains the following equation for  $q$  [4, 5]:

$$q = \frac{\Lambda + \chi\mu_p\mu_f}{K - \chi\mu_f^2}. \quad (18)$$

Let us now derive the same equation using the discrete model. Taking into account a coupling between the tilting order parameter and the spontaneous polarization, the free energy of the SmC\* phase can be written as [8, 11]:

$$F = \sum_j F_0(w_j^2) - \frac{1}{2}\eta(\mathbf{w}_j \cdot \mathbf{w}_{j+1}) - \frac{1}{2}b(\mathbf{w}_j \cdot \mathbf{w}_{j+1})^2 - \lambda(\mathbf{w}_j \times \mathbf{w}_{j+1} \cdot \mathbf{k}_0) + \frac{1}{2\chi}P_j^2 + c_p(\mathbf{w}_j \cdot \mathbf{P}_j) + \frac{1}{2}c_f(\mathbf{P}_j \times (\mathbf{w}_{j+1} - \mathbf{w}_{j-1}) \cdot \mathbf{k}_0) \quad (19)$$

where the last term describes the so called discrete flexoelectric effect which is discussed in detail in ref. [8]. The coefficients  $c_p$  and  $c_f$  are related to the piezo- and flexoelectric coefficients  $\mu_p$  and  $\mu_f$  of the continuum approach (16). Here the quadratic coupling term (the third term in eq.(19) with  $b > 0$ ) has been added to stabilize the system in the frustration region where  $\eta \approx 0$  (see below). On first sight the free energy (19) is rather different from the eq. (16). However, it can readily be shown that eq. (19) can be reduced to the same mathematical form as eq. (17) substituting the expansion of the order parameter  $\mathbf{w}_{j+1}$  given by eq. (5) and using the results of the previous subsection. For example, the flexoelectric term can be expanded as:

$$\begin{aligned} & \frac{1}{2}c_f(\mathbf{P}_j \times (\mathbf{w}_{j+1} - \mathbf{w}_{j-1}) \cdot \mathbf{k}_0) \\ & \approx -c_f((\mathbf{P}_j \times d \frac{\partial}{\partial z_j} \mathbf{w}_j) \cdot \mathbf{k}_0) \end{aligned}$$

$$= dc_f(\mathbf{P}_j \cdot (\mathbf{k}_0 \times \frac{\partial}{\partial z_j} \mathbf{w}_j)), \quad (20)$$

which exactly corresponds to the flexoelectric term in the continuum free energy (16). In a similar way one also obtains

$$\eta(\mathbf{w}_j \cdot \mathbf{w}_{j+1}) \approx \eta \left( 1 - \frac{1}{2} (\mathbf{w}_j \cdot \frac{\partial^2}{\partial z^2} \mathbf{w}_{j+1}) \right), \quad (21)$$

which takes the form of the elastic energy after integration by parts, and

$$\lambda(\mathbf{w}_j \times \mathbf{w}_{j+1}) \cdot \mathbf{k}_0 \approx \lambda(\mathbf{w}_j \cdot (\mathbf{k}_0 \times \frac{\partial}{\partial z_j} \mathbf{w}_j)), \quad (22)$$

which corresponds to the chiral term in the continuum free energy.

The minimization of the free energy (19) yields the following equation for the spontaneous polarization:

$$\begin{aligned} \mathbf{P}_j &= \chi \left( c_p \mathbf{w}_j + c_f d (\mathbf{k}_0 \times (\frac{\partial}{\partial z_j} \mathbf{w}_j)) \right) \\ &\approx \chi (c_p + 2c_f qd) \mathbf{w}_j. \end{aligned} \quad (23)$$

Substituting this equation back into the free energy (19) and using eq. (7) one obtains for the free energy density:

$$\begin{aligned} F/N &= F_0(\Theta) \\ &+ \frac{w_0^2}{N} \left( -\frac{1}{2} \eta - \frac{1}{2} b w_0^2 + \frac{1}{4} \eta (qd)^2 + b w_0^2 (qd)^2 + \lambda (qd) \right) \\ &- \frac{1}{2} \frac{\chi w_0^2}{N} \left( c_p^2 + 2c_p c_f qd + c_f^2 (qd)^2 \right). \end{aligned} \quad (24)$$

Finally minimization of (24) yields the equation for the helical pitch which has exactly the same mathematical form as eq. (18) obtained from the general continuum theory:

$$qd = \frac{\lambda + \chi c_p c_f}{\eta + 4b w_0^2 - \chi (c_f)^2}. \quad (25)$$

Here the quantity  $\eta$  corresponds to the dimensionless elastic konstant  $K/d^2$  in eq. (18),  $c_f$  corresponds to the dimensionless flexocoefficient  $\mu_f/d$  and  $c_p$  corresponds to  $\mu_p$ . Thus the discrete model yields essentially the same expression for the helical pitch as the general continuum theory.

The magnitude of the parameter  $\eta$  decreases on approaching the synclinic–antclinic phase transition and at the transition point  $\eta = 0$ . Thus, without a sufficiently large quadratic

coupling constant  $b$  the effective elastic constant (i.e. the denominator in eq. (25)) will become negative at some point *within* the SmC\* phase close to the transition point, and for  $\eta = 2\chi(c_f)^2$  the pitch would become zero. The quadratic coupling term stabilizes the system in this region accounting for the positive values of the effective elastic constant. It should be noted, however, that the term  $4bw_0^2$  may become negligibly small close to the transition into the untilted SmA\* phase. In this regime, where the magnitude  $w$  of the tilt order parameter is very small, the effective dimensionless elastic constant  $K_{eff} = \eta + 4bw_0^2 - 2\chi(c_f)^2$  may, in principle, become very close to zero or even negative for some materials if the parameter  $\eta$  is small.

One notes that the point where the effective elastic constant  $K_{eff}$  vanishes corresponds to the absolute limit of stability of the macroscopic helical structure with pitch in the typical range of the SmC\* and SmC<sub>a</sub>\* phases ( $\sim 0.5\mu\text{m}$  or longer). Above this point a different helical structure with very short pitch may occur, which may not be described using the expansion in powers of  $qd$  used in this paper. This may explain the origin of the SmC <sub>$\alpha$</sub> \* phase, the main characteristics of which are an extremely short pitch and small tilt angle. The latter is due to the fact that the phase – when it appears – always forms following a second-order transition from SmA\* and that its temperature range is small, typically less than 5 K. Furthermore, the SmC <sub>$\alpha$</sub> \* phase appears only in AFLCs, i.e. in materials exhibiting the SmC<sub>a</sub>\* phase with  $\eta < 0$  at low temperatures. Since SmC <sub>$\alpha$</sub> \* is not anticlinic,  $\eta$  must change sign between this phase and SmC<sub>a</sub>\*. If this sign change is close to the low-temperature limit of SmC <sub>$\alpha$</sub> \* the magnitude of  $\eta$  as well as the tilt should be small within this phase. Hence it is not unlikely that the requirements for  $K_{eff} < 0$  are fulfilled, thereby explaining why SmC <sub>$\alpha$</sub> \* rather than the ordinary SmC\* phase forms.

An experiment which supports this line of reasoning was published by Isozaki et al. [12]. By reducing the optical purity of the compound TFMHPOCBC, which in its optically pure state exhibits a direct SmA\*–SmC<sub>a</sub>\* transition (thus having  $\eta < 0$  at all temperatures below the onset of tilt) the SmC <sub>$\alpha$</sub> \* phase was induced over the interval between 80% and 60% enantiomeric excess. On further racemization the SmC\* phase appeared, first below SmC <sub>$\alpha$</sub> \*, then directly below SmA\*. Obviously the reduction of optical purity continuously shifts the balance between syn- and anticlinicity away from the strictly anticlinic case of the optically pure compound. In other words,  $\eta$  increases. At a certain amount of the opposite enantiomer,  $\eta$  changes sign within the temperature range of non-zero tilt. Thus, over a certain interval

of enantiomeric excess,  $\eta$  will be small but positive at high temperatures, where the tilt is small. According to the model the ordinary SmC\* phase is then unstable, explaining the appearance of SmC $_{\alpha}$ \*. As the optical purity is further reduced the temperature where  $\eta$  changes sign decreases. As a result,  $\eta$  is no longer small in the region of small tilt and SmC $_{\alpha}$ \* is replaced by SmC\*.

### C. Helical pitch of the anticlinic SmC $_{\alpha}$ \* phase

In the discrete model the free energy of the anticlinic SmC $_{\alpha}$ \* phase is given by the same eq. (19) but with negative sign of the parameter  $\eta$ . Minimization yields an equation for the spontaneous polarization:

$$\mathbf{P}_j = \chi c_p \mathbf{w}_j + \chi \frac{1}{2} c_f (\mathbf{k}_0 \times (\mathbf{w}_{j+1} - \mathbf{w}_{j-1})). \quad (26)$$

Using eq. (12) and the corresponding equation for the order parameter in the layer  $j - 1$ :

$$\mathbf{w}_{j-1} = -\mathbf{w}_j + d \frac{\partial}{\partial z_j} \mathbf{w}_j - \frac{1}{2} d^2 \frac{\partial^2}{\partial z_j^2} \mathbf{w}_j + \dots, \quad (27)$$

the polarization (26) can be expanded as

$$\begin{aligned} \mathbf{P}_j &\approx \chi \left( c_p \mathbf{w}_j - d c_f (\mathbf{k}_0 \times \left( \frac{\partial}{\partial z_j} \mathbf{w}_j \right)) \right) \\ &\approx \chi (c_p - 2d q c_f) \mathbf{w}_j. \end{aligned} \quad (28)$$

Substituting eq. (28) into the free energy (19) and using eq. (13) one obtains

$$\begin{aligned} F/N &= F_0(\Theta) \\ &+ \frac{w_0^2}{N} \left( -\frac{1}{2} \eta - \frac{1}{4} \eta (qd)^2 + b w_0^2 (qd)^2 - \lambda (qd) \right) \\ &- \frac{1}{2} \frac{\chi w_0^2}{N} (c_p^2 - 2c_p c_f q + c_f^2 q^2). \end{aligned} \quad (29)$$

where  $\eta < 0$ . The expression for the helical pitch of the anticlinic SmC $_{\alpha}$ \* phase is obtained by minimization of the free energy density (29):

$$qd = -\frac{\lambda + \chi c_p c_f}{|\eta| + 4b w_0^2 - \chi (c_f)^2}, \quad (30)$$

Comparing eqs. (30) and (25) one concludes that the sense of the helical pitch in the anticlinic SmC $_{\alpha}$ \* phase should be opposite to that in the synclinic phase also if the coupling

between the tilt order parameter and the polarization is taken into account. In the simple model used here the absolute value is unaffected by the transition, a situation which only rarely occurs in reality. This discrepancy may possibly be related to long-range interactions between layers, neglected in the present model. We have deliberately restricted our analysis to interactions between adjacent layers in order to present simple analytical expressions for the helical wave vector, from which one can qualitatively understand the change of handedness at the phase transition. In more complex models, including long-range interactions, the pitch can only be calculated numerically [8, 13]. Such calculations yield different absolute values of the pitch in the two phases but always – as in the present model – a change of handedness.

### III. EXPERIMENTS AND OBSERVATIONS

#### A. Strategy

The opposite handedness of the helix in the  $\text{SmC}^*$  and  $\text{SmC}_a^*$  phases of a single compound exhibiting both these phases is well documented experimentally (see e.g. references [1–3]). In Figure 1 we give a demonstration, using the example of (*S*)-12F1M7 (cf. Table I), an AFLC compound exhibiting the  $\text{SmC}^*$  as well as the  $\text{SmC}_a^*$  phase, with similar pitch magnitudes [14]. The photos show the homeotropic texture in the two phases viewed in transmission in the polarizing microscope, illuminated with blue light (436 nm), between crossed (centre column) and slightly decrossed polarizers. The selective reflection wavelength is  $\sim 480$  nm in  $\text{SmC}_a^*$  and  $\sim 450$  nm in  $\text{SmC}^*$ , hence the same branch of the optical rotation function is studied in both cases. The opposite relations between polarizer decrossing sense and transmission change in the two phases show that they have opposite helix sense.

INSERT FIGURE 1 ABOUT HERE

Rather than studying single-component AFLCs with  $\text{SmC}^*$  and  $\text{SmC}_a^*$  phases, we have in this work chosen to look at mixture-induced transitions between the phases. We have previously demonstrated [15] that the mixing of strictly synclinic compounds with strict anti-

clinics induces a clinicity frustration which the system can resolve in one of three alternative ways:

1. direct change between  $\text{SmC}^*$  and  $\text{SmC}_a^*$  at a specific mixture ratio
2. the intermediate chiral smectic-C phases  $\text{SmC}_\beta^*$  and  $\text{SmC}_\gamma^*$  are induced over a range of mixture ratios close to 50:50
3. the temperature range of the non-tilted  $\text{SmA}^*$  phase is expanded downwards such that it separates the syn- and anticlinic phases in the phase diagram.

Mixtures following the first two paths provide excellent experimental systems for comparing with the theoretical predictions described above. By studying contact samples between the two components we can in general observe the whole phase sequence at a single temperature and we can thus easily make direct comparisons between the  $\text{SmC}^*$  and  $\text{SmC}_a^*$  phases, without the need for a controlled temperature gradient. Furthermore, we can choose the handedness of the  $\text{SmC}^*$  phase irrespective of that of the  $\text{SmC}_a^*$  phase, since each is set by a different mesogen. This allows for the generation of some quite interesting effects, as will be described below.

## B. Experimental details

The compounds used for the study are summarized in Table I together with their phase sequences. For simplicity the study was restricted to (*S*)-enantiomers of all mesogens (in one case to the (*S,S*)-stereoisomer). Contact samples were prepared between selected syn- and anticlinics on ordinary microscope slides. If homeotropic alignment did not occur spontaneously the slide was coated with a surfactant (CTAB) or with a very thin layer of grease, ensuring fully homeotropic alignment.

INSERT TABLE ABOUT HERE

Textures were investigated in transmission in an Olympus BH-2 polarizing microscope and photographed using a Nikon Coolpix digital camera mounted on the photo tube of the microscope. The samples were inserted into an Instec Mk2 hotstage mounted on the microscope table for accurate temperature control.

### C. Experimental observations

In all cases when the two components have opposite helix sense, i.e. the synclinic is right-handed and the anticlinic left-handed, or vice versa (this is the usual case for components of the same enantiomeric type), the twisting sense reversal was found to take place at the transition between  $\text{SmC}^*$  and  $\text{SmC}_a^*$  or within the intermediate  $\text{SmC}_\beta^*$  and  $\text{SmC}_\gamma^*$  phases. In the first two rows of Figure 2, two examples of polarizing microscopy texture sets demonstrating this connection of helix inversion and clinicity transition, via intermediate phases (a) and directly (b), are shown. The opposite helix sense on the two sides of the transition is verified by decrossing the polarizers, producing more saturated colors for one twisting sense but a brighter texture with washed-out colors for the other. In contrast to a helix inversion within a single phase there is here no pitch divergence connected to the twisting sense reversal. Rather the contrary phenomenon was actually observed in most cases: as the mixing ratio was shifted towards the transition composition at a particular temperature, the pitch tightened. This happened almost always in the  $\text{SmC}^*$  region and often also in the  $\text{SmC}_a^*$  phase. Although apparent in Figure 2 b the effect is seen better in the examples of Figure 3 where the changes in color clearly demonstrate how the pitch is changing.

INSERT FIGURE 2 ABOUT HERE

INSERT FIGURE 3 ABOUT HERE

On the other hand, if the syn- and anticlinic components each on their own have the same helix twisting sense, we create an additional type of frustration, since the helix sense has to revert at the syn- to anticlinic transition as shown in Section II. We do not need to switch to the opposite enantiomer of one of the components – thereby strongly changing the situation with respect to chiral interactions, with obvious consequences for both helix and spontaneous polarization – to reach this situation, but we can induce it by choosing one component with a trifluoromethyl group instead of methyl at the stereogenic center. For one and the same phase, the helix handedness of a methyl- and a trifluoromethyl-containing compound is opposite, hence the handedness of a non-fluorinated synclinic and a fluorinated anticlinic is the same.

The interesting way in which nature decides to resolve this frustration can be seen in Figure 2 c, where the anticlinic is the well-studied trifluoromethyl-containing antiferroelectric liquid crystal TFMHPOBC. At the phase transition point the helix diverges but there is no change in helix sense at any place, as is obvious from the photos with decrossed polarizers. By making the helical pitch infinite, where left- and right-handed are degenerate, the system can fulfill both—seemingly incompatible—constraints that the helix sense has to change at a syn- to anticlinic transition, and that both components each on their own has the same helix sense. Whereas pitch divergence within a single phase is generally connected to a helix sense reversal, in the case of mixtures of syn- and anticlinics we have divergence in the *absence* of reversal, whereas the pitch generally *shortens* on approaching the ordinary transition between syn- and anticlinic order with helix sense reversal. These two cases are illustrated very schematically in Figure 4.

INSERT FIGURE 4 ABOUT HERE

The strong influence on the pitch which the combination of syn- and anticlinics has might be put to use when developing mixtures for FLC or AFLC displays. In most cases the pitch should preferably be long in order to ensure complete surface stabilization. By choosing anticlinic and synclinic components with the same helix handedness, which do not generate intermediate phases or extend the SmA\* phase when mixed together, one forces the system to undergo a pitch divergence on approaching the clinicity change. The mixture ratio should be selected as close as possible to the point of clinicity change, but of course sufficiently far away to ensure that only the desired phase, SmC\* or SmC<sub>a</sub>\*, appears in the phase sequence. On the other hand, for devices utilizing the deformed helix mode a SmC\* phase with very short pitch is required. This can then be obtained by choosing components with opposite helix handedness in their pure states [16].

#### IV. CONCLUSIONS

By studying the free energy of the helical SmC\* and SmC<sub>a</sub>\* phases within a discrete phenomenological model we have shown that the helix handedness in the two phases should be opposite. The discrete model produces essentially the same expression for the helical

pitch of the  $\text{SmC}^*$  phase as the general continuum theory. Using the same discrete model we have also obtained the expression for the pitch in the anticlinic antiferroelectric  $\text{SmC}_a^*$  phase. These equations indicate that the helical pitch should decrease on approaching the synclinic-anticlinic transition provided that the tilt angle does not vary strongly in the transition region. It was also shown that in chiral smectics exhibiting a transition between syn- and anticlinic tilted order, the helical structure with normal pitch (on the order of  $\mu\text{m}$ ) may lose its stability if the synclinic temperature range is small, such that the transition takes place close to the low-temperature border of the  $\text{SmA}^*$  phase, where the tilt angle is small. This may be an indication of a transition into the  $\text{SmC}_\alpha^*$  phase.

The theoretically predicted helix handedness reversal related to a change between syn- and anticlinic order was demonstrated experimentally by studying mixtures of strict syn- and anticlinic mesogens where the clinicity transition takes place at a certain mixture ratio, either directly or via induced intermediate  $\text{SmC}_\beta^*$  and  $\text{SmC}_\gamma^*$  phases. If one chooses two components which have the same helix handedness each on their own, although one of them is synclinic and the other one anticlinic, the system lets the pitch diverge at the clinicity transition, such that the requirement of helix reversal can still be fulfilled, as left- and right-handed helices are degenerate at infinite pitch.

This paper is dedicated to Sven T. Lagerwall at the occasion of his 70<sup>th</sup> birthday.

## V. ACKNOWLEDGMENTS

J.L. gratefully acknowledges financial support from the Alexander von Humboldt Foundation. The samples of liquid crystalline compounds used for the experimental part were kindly provided by Prof. G. Heppke, TU-Berlin, Germany.

- 
- [1] A. Chandani, E. Gorecka, Y. Ouchi, H. Takezoe, and A. Fukuda, *Jap. J. Appl. Phys.* 2 **28**, L1265 (1989).
  - [2] J. Li, H. Takezoe, and A. Fukuda, *Jap. J. Appl. Phys.* 1 **330**, 532 (1991).
  - [3] P. Gisse, V. L. Lorman, J. Pavel, and H. T. Nguyen, *Ferroelectrics* **178**, 297 (1996).
  - [4] S. A. Pikin and V. L. Indenbom, *Sov. Phys. Usp.* **21**, 487 (1979).
  - [5] S. A. Pikin and V. L. Indenbom, *Ferroelectrics* **3-420**, 151 (1978).

- [6] M. A. Osipov and S. A. Pikin, *J. Phys. (Paris) II* **85**, 1223 (1995).
- [7] D. Olson, X. Han, A. Cady, and C. Huang, *Phys. Rev. E* **266**, 021702 (2002).
- [8] A. Emelyanenko and M. Osipov, *Phys. Rev. E* **68**, 051703 (2003).
- [9] R. Bruinsma and J. Prost, *J. Phys. (Paris) II* **74**, 1209 (1994).
- [10] P. Mach, R. Pindak, A. M. Levelut, P. Barois, H. T. Nguyen, C. C. Huang, and L. Furenlid, *Phys. Rev. Lett.* **81**, 1015 (1998).
- [11] M. Cepic and B. Zeks, *Phys. Rev. Lett.* **87**, 085501/1 (2001).
- [12] T. Isozaki, H. Takezoe, A. Fukuda, Y. Suzuki, and I. Kawamura, *J. Mater. Chem.* **4**, 237 (1994).
- [13] M. Cepic, E. Gorecka, D. Pocięcha, B. Zeks, and H. Nguyen, *J. Chem. Phys.* **117**, 1817 (2002).
- [14] J. P. F. Lagerwall, D. D. Parghi, D. Krüerke, F. Gouda, and P. Jägemalm, *Liq. Cryst.* **29**, 163 (2002).
- [15] J. P. F. Lagerwall, G. Heppke, and F. Giesselmann, Submitted to *Eur. Phys. J. E* (2005).
- [16] J. P. F. Lagerwall, *Phys. Rev. E* **71**, 051703 (2005).

## Figure captions

1. A homeotropically aligned sample of (*S*)-12F1M7 in the SmC\* phase (top row) and SmC<sub>a</sub>\* phase (bottom row), observed in transmission in a polarizing microscope illuminated with blue light (436 nm), between crossed and slightly decrossed polarizers, as indicated at the bottom left of each photo.
2. Homeotropically aligned contact samples between synclinics and anticlinics where the clinicity transition takes place via the intermediate SmC<sub>β</sub>\* and SmC<sub>γ</sub>\* phases (a) and directly (b and c). In the middle column the polarizers are crossed, in the left and right they are decrossed as indicated at the bottom left of each photo. This visualizes the helix handedness reversal in (a) and (b) (SmC\* gets darker when SmC<sub>a</sub>\* gets brighter and vice versa) and the constance in handedness in c (both phases get brighter or darker for the same type of polarizer decrossing).
3. Homeotropically aligned contact samples between synclinics and anticlinics where the clinicity transition takes place via subphases (a and b) and directly (c), in all cases with a drastic decrease in SmC\* pitch on approaching the transition. In cases (a) and (b) this holds also for the SmC<sub>a</sub>\* phase.
4. Sketches of the typical behavior of the pitch (*p*) as the temperature (*T*) or mixture composition (*x*) is varied, such that a transition between syn- and anticlinic order takes place. The standard behavior is a helix handedness change with pitch decrease on approaching the transition – case (a) – but by smart mixing we can also get case (b), where the pitch diverges at the transition but the handedness remains the same.

## Table captions

1. Compounds used in the study. Transition temperatures in °C.

## Figures

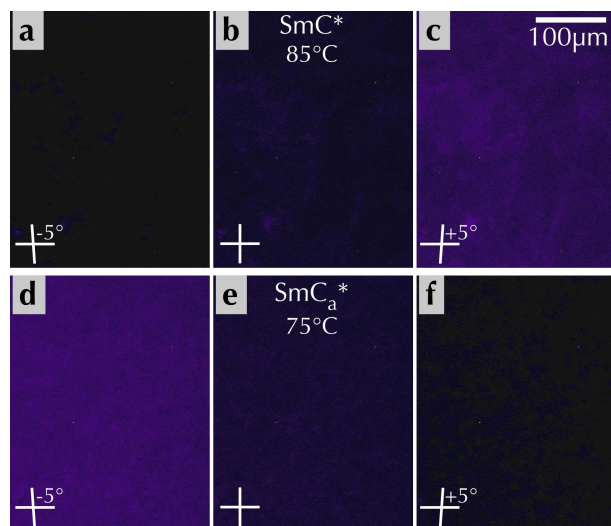


FIG. 1:

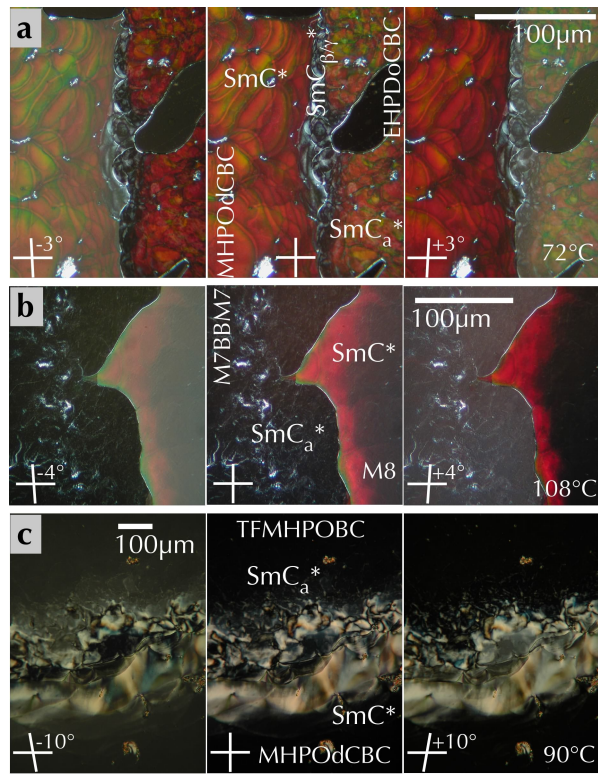


FIG. 2:

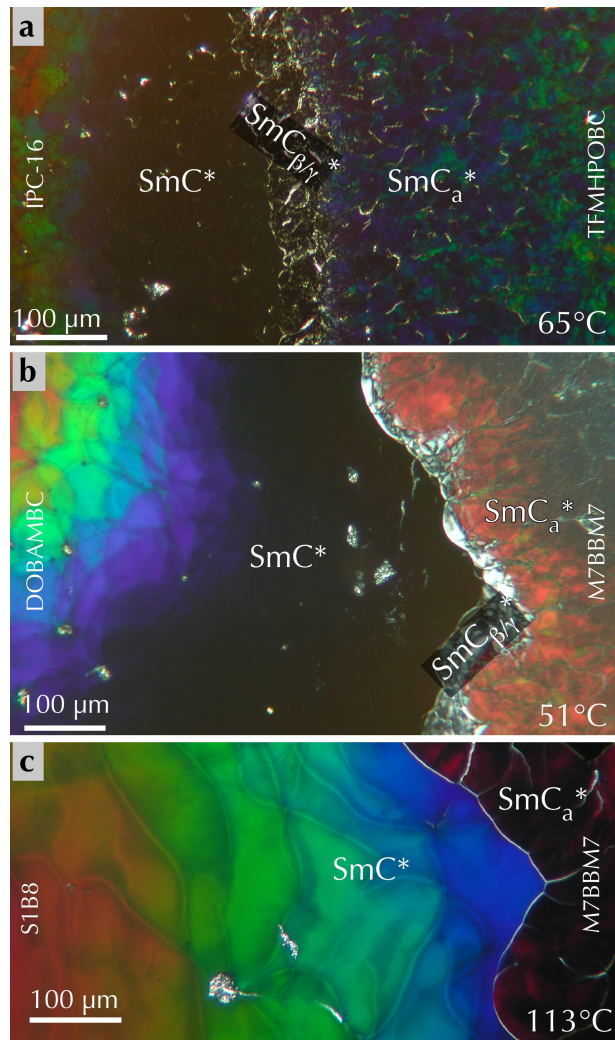


FIG. 3:

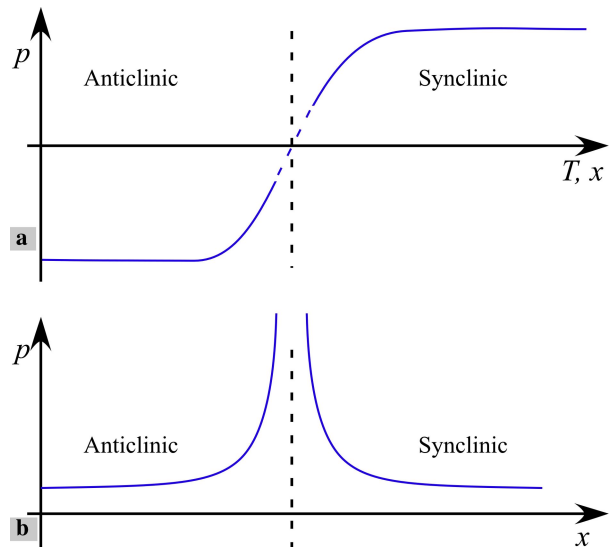
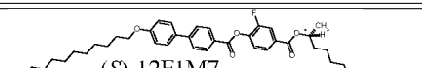
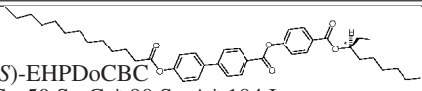
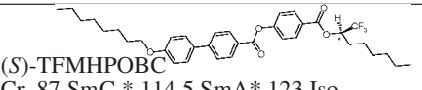
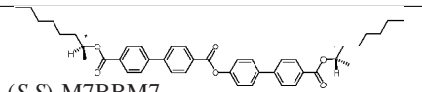
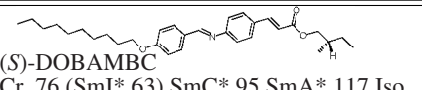
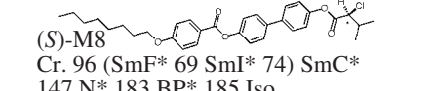
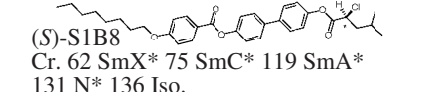
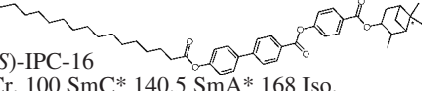
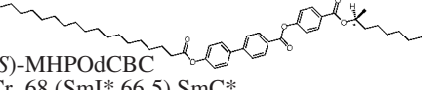


FIG. 4:

## Tables

TABLE I:

<i>Name, structure and phase sequence</i>	<i>Type</i>
 <p>(S)-12F1M7 SmC<sub>a</sub>* 79.5 SmC<sub>γ</sub>* 83 SmC<sub>β</sub>* 85 SmC* 92 SmA* 110 Iso.</p>	syn- & anticlinic
 <p>(S)-EHPDoCBC Cr. 50 SmC<sub>a</sub>* 90 SmA* 104 Iso.</p>	anticlinic
 <p>(S)-TFMHPOBC Cr. 87 SmC<sub>a</sub>* 114.5 SmA* 123 Iso.</p>	anticlinic
 <p>(S,S)-M7BBM7 Cr. 57 SmC<sub>a</sub>* 65 SmQ* 85 Iso.</p>	anticlinic
 <p>(S)-DOBAMBC Cr. 76 (SmI* 63) SmC* 95 SmA* 117 Iso.</p>	synclinic
 <p>(S)-M8 Cr. 96 (SmF* 69 SmI* 74) SmC* 147 N* 183 BP* 185 Iso.</p>	synclinic
 <p>(S)-S1B8 Cr. 62 SmX* 75 SmC* 119 SmA* 131 N* 136 Iso.</p>	synclinic
 <p>(S)-IPC-16 Cr. 100 SmC* 140.5 SmA* 168 Iso.</p>	synclinic
 <p>(S)-MHPOdCBC Cr. 68 (SmI* 66.5) SmC* 114 SmA* 124 Iso.</p>	synclinic